

See discussions, stats, and author profiles for this publication at: <https://www.researchgate.net/publication/220002276>

# Direct visualisation of micelles of Pluronic block copolymers in aqueous solution by cryo-TEM

ARTICLE *in* PHYSICAL CHEMISTRY CHEMICAL PHYSICS · JULY 1999

Impact Factor: 4.49 · DOI: 10.1039/A902369K

---

CITATIONS

53

---

READS

200

## 3 AUTHORS:



**Yeng-Ming Lam**

Nanyang Technological University

108 PUBLICATIONS 2,873 CITATIONS

SEE PROFILE



**Nikolaus Grigorieff**

Howard Hughes Medical Institute

100 PUBLICATIONS 7,260 CITATIONS

SEE PROFILE



**Gerhard Goldbeck**

Goldbeck Consulting Limited

76 PUBLICATIONS 1,151 CITATIONS

SEE PROFILE

# Direct visualisation of micelles of Pluronic block copolymers in aqueous solution by cryo-TEM

Yeng-Ming Lam,<sup>a</sup> Nikolaus Grigorieff<sup>†b</sup> and Gerhard Goldbeck-Wood<sup>a</sup>

<sup>a</sup> Department of Materials Science and Metallurgy, University of Cambridge, Pembroke Street, Cambridge, UK CB2 3QZ

<sup>b</sup> MRC Laboratory of Molecular Biology, Hills Road, Cambridge, UK CB2 2QH

Received 24th March 1999, Accepted 28th May 1999

Micelles formed by (ethylene oxide) (propylene oxide) (ethylene oxide) triblock copolymers (Pluronic F127 and L64) in aqueous solutions have been visualised by cryogenic transmission electron microscopy (cryo-TEM). The resolution achieved allows detailed inspection of the individual micelles, their size, shape, core-shell structure as well as long-range order. The dependence of the microstructure on the concentration of the solution as well as on the type (block sizes) of the Pluronic polymer are reported and demonstrate the sensitivity of the method to these parameters.

## Introduction

Micelle forming, amphiphilic block copolymers have a number of interesting applications ranging from non-ionic surfactants in cleaning liquids to drug carriers for hydrophobic pharmaceuticals.<sup>1–3</sup> In many of these applications direct information about the structure of individual micelles and their microstructural arrangement is important for the control of properties. Pluronic, (ethylene oxide) (propylene oxide) (ethylene oxide) triblock copolymers, are a technologically important, and hence widely studied, representative of the class of amphiphilic block copolymers. In a previous study,<sup>4</sup> the cryogenic transmission electron microscopy method was applied to the Pluronic F127. The micrographs shown in ref. 4 only just allow the rows of micelles to be discerned as dark dots. Although these results reveal the basic structural elements of micellar arrangement, the imaging and resolution does not allow the individual micellar size and shape to be analysed. In the following we report on a preliminary cryo-TEM study of solutions of two different Pluronic polymers at two different concentrations which demonstrates that the method allows individual micelles and their microstructure to be visualised very clearly. The method hence lends itself to much more detailed studies of micellisation which will be the focus of further work.

## Materials

The materials used in the present study are two (ethylene oxide) (propylene oxide) (ethylene oxide) or (EO)<sub>m</sub>(PO)<sub>n</sub>(EO)<sub>m</sub> triblock copolymers of compositions:  $m = 99$ ,  $n = 65$  and  $m = 13$ ,  $n = 30$ , respectively. The former is designated F127, the latter L64. Both materials were obtained from Fluka, and have been used without further purification. A similar, but not identical, material (Synperonic PE/F127 from ICI Specialties) was previously studied by Yu *et al.*<sup>5</sup>

The F127 and L64 materials were dissolved by weight in distilled water at 5 °C and incubated at various temperatures for 24 h before being used in the experiments described below.

## Methods

### Differential scanning calorimetry (DSC)

DSC has been used to estimate the range of temperatures over which micellisation occurs for a particular concentration. As micellisation is a first order transition, the endothermic effect of micellisation can be observed clearly when looking at the first derivative of the heat of reaction, which is proportional to heat capacity. For the measurements a Perkin Elmer DSC 7 system was used, calibrated by standard procedures. The aqueous samples were placed in hermetically sealed aluminium pans. The scans were carried out in a nitrogen environment at a constant heating rate of 10 °C min<sup>-1</sup>, covering the range of 5 to 90 °C. To check on the validity of the measured micellisation temperatures, we also carried out a heating and cooling cycle at a rate of 2 °C min<sup>-1</sup>.

### Electron cryo-microscopy

Perforated carbon films were prepared following a procedure described by Bradley.<sup>6</sup> Briefly, a Formvar plastic film was produced by drying a thin film of 0.5% Formvar solution in chloroform containing a suspension of water-glycerol (ratio 1 : 1 v/v) droplets on a glass slide. The film was then floated off the slide and 400-mesh copper-rhodium grids were placed on the film. The film together with the grids was lifted quickly off the water surface by adhesion to a filter paper. Then the filter paper was soaked in methanol for 5 to 10 min, thereby producing holes in the plastic film. Carbon was evaporated onto the holey Formvar film, and then the plastic was dissolved in chloroform. The polymer solution was generally kept at about 30 °C (F127) and about 40 °C (L64) before freezing. In one case an L64 sample was prepared at room temperature for comparison. Samples were frozen according to the following procedure.<sup>7</sup> Solution (2 µl) was applied while the grid was mounted in a controlled environment freezing apparatus maintained at 50 °C and very high humidity.<sup>8</sup> After 30 s the grid was blotted from the carbon side for 5–10 s with a double layer of filter paper (Whatman no. 1) before plunging it into liquid ethane. Images of micelles in ice over holes in the carbon film were recorded under low-dose conditions (electron dose was about 10 e<sup>-</sup>/Å<sup>2</sup>), from untilted samples at a

<sup>†</sup> Present address: Rosenstiel Center—MS 029, Brandeis University, 415 South Street, Waltham, MA 02454-9110, USA

magnification of  $60\,000\times$  on a Philips CM12 electron microscope running at 120 keV, and fitted with a tungsten filament electron source. The microscope was equipped with a Gatan cold stage to keep the sample at liquid nitrogen temperature. The defocus in the images was 0.5 to 1.0  $\mu\text{m}$ .

### Image analysis of electron micrographs

Image processing is now commonly used in various aspects of electron microscopy such as three dimensional reconstruction from two dimensional images, extraction of signal from noisy images and also feature quantification.<sup>9</sup> There are various commercial software packages available for these tasks. We have used the *Semper* software to process and analyse the micrographs.

The analysis is performed on a scan of the micrograph of a particular sample. After Fourier transformation of the image data, the significant feature in the transformed image is further enhanced. A statistical calculation is then carried out on a fixed area specified by the user and information regarding feature size, periodicity, frequency and diffraction patterns is extracted.

### Results and discussion

The following three samples were prepared as described above: F127, 10%; F127, 5%, L64, 10%. Characterisation by means of DSC of the different solutions provided the critical micellisation temperatures shown in Tables 1 and 2. Generally, micellisation is marked by a small increase in measured enthalpy which is observed as a small peak in the specific heat capacity for both F127 and L64. The transition enthalpies of 20–30  $\text{J g}^{-1}$  are consistent with previously measured values,<sup>5</sup> as are the observed micellisation temperatures. As expected in a system with long relaxation times, the peak was observed at a 2 to 3  $^{\circ}\text{C}$  lower temperature at the slower heating rate of  $2^{\circ}\text{C min}^{-1}$ , and on cooling a small exothermic peak was observed about 5  $^{\circ}\text{C}$  below the heating peak. In addition, we have confirmed these observations by other indirect methods such as photon correlation spectroscopy, viscometry and small angle X-ray scattering. The main point, however, is that the DSC allows us to put an upper bound on the micellisation transition which provides us with a 'safe' temperature at which to prepare samples for the cryo-TEM observation of micelles.

The resulting TEM images for vitrified specimens of F127 at 10 and 5% concentration and vitrified specimens of L64 at 10% concentration are shown in Figs. 1–3, respectively. The field of view approximately covers the area of one hole in the film covering the grid. In each such hole in each vitrified specimen we observe a gradient in thickness of the specimen across the hole. One can see a single layer of spherical micelles in the centre, and two or more layers of micelles overlapping closer to the edge.

The micro-phase separated structures are clearly visualised due to the contrast achieved by the defocus. In each case, a

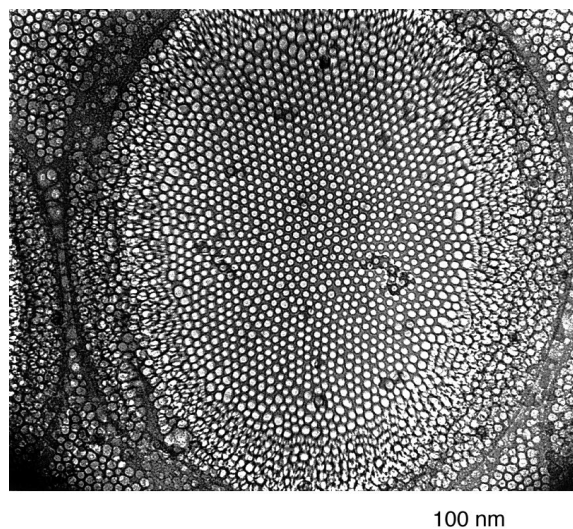


**Fig. 1** Electron micrograph of a vitrified sample of 10% F127 solution.

structure which is consistent with a micellar phase is observed, in agreement with previous work.<sup>4,10</sup> The structures are unlikely to be cuts through rods since such elongated shapes would tend to lie flat in a thin layer as the one observed here.

Individual micelles can be distinguished particularly well on the micrographs of the F127 samples (Figs. 1 and 2). They are generally spherical in shape and exhibit a core-shell structure. By careful inspection one can distinguish between the brighter

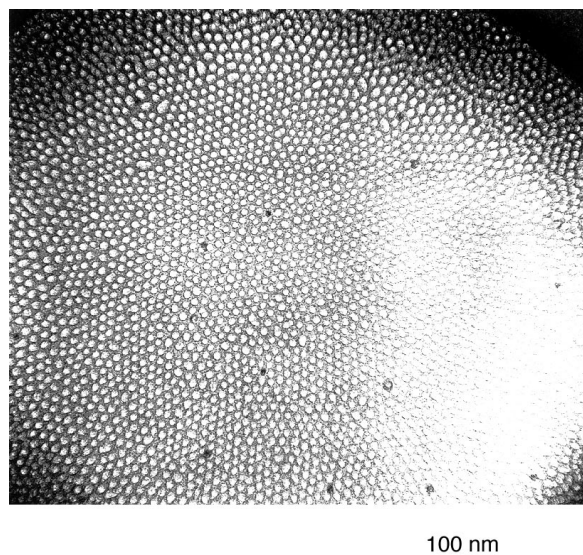


**Fig. 2** Electron micrograph of a vitrified sample of 5% F127 solution.

**Table 1** Critical micellisation temperature (CMT) variation with concentration for F127 measured during heating at  $10^{\circ}\text{C min}^{-1}$

Concentration (wt.%)	20	10	8	6	4	2
CMT/ $^{\circ}\text{C}$ —onset	14	20	21	23	24	25
Peak temperature	18	22	24	25	26	28

The peak temperature refers to the temperature at which the maximum heat flow occurred.

**Table 2** Critical micellisation temperature variation with concentration for L64

Concentration (wt.%)	20	10	5	1
CMT/ $^{\circ}\text{C}$ —onset	21	28	31	36
Peak temperature	29	34	37	39

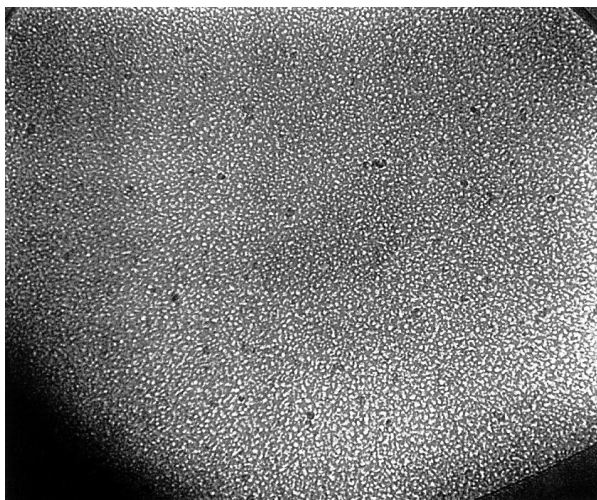


**Fig. 3** Electron micrograph of a vitrified sample of 10% L64 solution.

core of the micelles, and the dark shell, surrounded by a matrix of intermediate grey tone. The bright rings, or sometimes half rings, which can be seen between the core and the shell of some micelles are Fresnel fringes. This observation is clearly consistent with the micelles consisting of a hydrophobic poly(propylene oxide) core and a shell comprising poly(ethylene oxide) and water. The core appears to be lighter because of the lower electron density as compared to the shell where water is present. In contrast, a sample of L64 prepared at room temperature, *i.e.* below the critical micellisation temperature of the given solution, showed no evidence of micelles.

The volume fractions of micelles in the micrographs appear much higher than the concentrations in the original solutions. This is a direct result of the sample preparation. Blotting the grids immediately before plunging them into liquid ethane leads to a preferential removal of solvent.

Furthermore, the vitrified samples of the F127 solutions exhibit a degree of hexagonal order of the micelles which is elucidated by the diffraction patterns in Figs. 4a and b. In particular the 10% sample shows considerable long range order. As above we believe this ordering to be a result of the removal of excess water during the sample preparation which leads to a locally denser packing of the micelles. We note, however, that at the given temperatures F127 is known to form a mesophase of cubic packed spheres for concentrations above about 25 wt.%.<sup>3</sup>

The increase in the degree of order between the 5 and 10% F127 samples is also consistent with the evidence from small angle neutron scattering (SANS)<sup>4</sup> which shows an increase in spatial correlation between the micelles with concentration.

In the case of the L64 sample the arrangement of the micelles looks more random. In contrast to the F127 case many micelles appear to be elongated rather than spherical in shape. We note, as above, that at the given temperatures L64 first forms a mesophase of hexagonally packed cylinders at a concentration of about 40 wt.%.<sup>3</sup>

The statistical analysis of the micellar sizes by means of the *Semper* software provides the size distribution of the F127 micelles as shown in Figs. 5 and 6. The size of the micelle core in the 5 and 10% solution is approximately about 6.0 and 10.8 nm in diameter, respectively. The size distribution of the 10% F127 sample is somewhat bimodal with a significant population in the range 6–7 nm. This may be due to the fact that the molecular weight distribution of F127 is in fact bimodal.<sup>5</sup> Gel permeation chromatography (GPC) using THF as a solvent<sup>11</sup> shows that about 80% of material is of a molecular

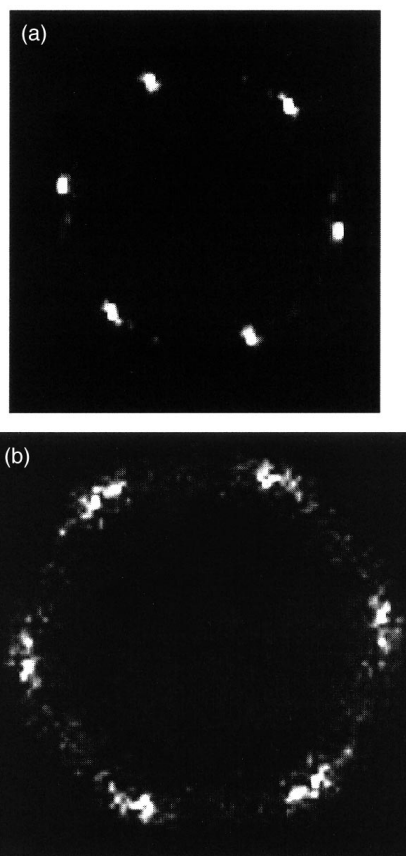


**Fig. 4** Diffraction patterns obtained from the *Semper* analysis: (a) of 10% F127, (b) of 5% F127.

weight close to the formula weight of 12549, while the remaining 20% has a weight of about 4000.

The core size of the micelles at 5% agrees exactly with that derived by Mortensen and Talmon from their SANS data.

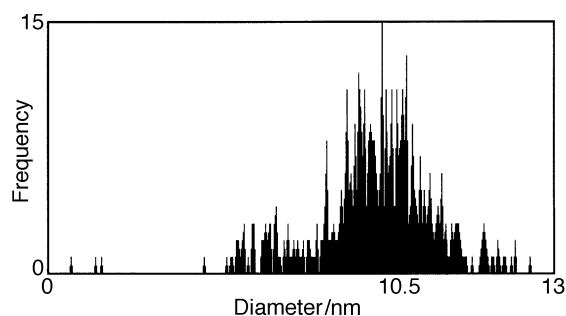


**Fig. 5** Histogram of size distribution of micelles for 10% F127. The mean diameter is approximately 10.8 nm.

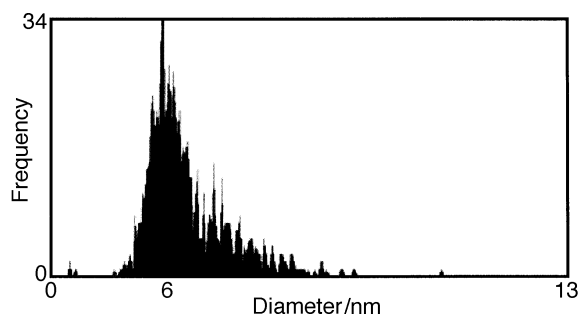


**Fig. 6** Histogram of the size distribution of micelles for 5% F127. The mean diameter is approximately 6 nm.

However, in contrast to our observation they reported only a weak dependence of size on concentration, without actually providing a value for concentration larger than 5%. The significant difference in size in the two different concentrations may be attributed to the fact that the PO segments experience at low concentration more strongly the poor solvent quality of the water and hence tend to undergo 'collapse transition.' The core diameter is in fact just a quarter of the length of the 65 monomer PO block in *trans*-planar conformation, which is 23.8 nm, whereas it is about half that in the case of the 10% solution.

On the basis of the core size for F127 we can calculate the aggregation number of the micelles.<sup>1</sup> The volume of the PO block is  $6.123 \times 10^{-21} \text{ cm}^3$ , as derived by the *Synthia* module from the Cerius<sup>2</sup> software by Molecular Simulations Inc. Assuming that the core is entirely made up of the PO blocks, the aggregation number is 18 for the 5% solution and 108 for the 10% solution.

In the case of the 10% L64 solution a similar statistical analysis could not be carried out because of insufficient contrast. Visual inspection of the micrograph, Fig. 3, nevertheless reveals micelles with a bright core. The typical core size is about 4–6 nm, which is about half the size of the PO *trans*-planar segment length of 11.0 nm, *i.e.* in the same proportion as for the 10% F127 solution. The resulting aggregation number is about 20–30.

## Conclusions and further work

We have shown that the cryo-TEM of vitrified aqueous solutions of block-copolymers can provide a clear and detailed visualisation of Pluronic micellar systems. We have identified the core-shell structure, and analysed the micellar ordering and structure of the individual micelle. We have found good comparison with other indirect techniques. In future we plan to extend the study to other micro-phase separated structures,

further amphiphilic materials, and micellar drug delivery systems.

## Acknowledgements

We would like to acknowledge financial support for this work by Nanyang Technological University, Singapore, and thank Molecular Simulations Inc. for providing the Cerius<sup>2</sup> software.

## References

- 1 C. E. Fairhurst, S. Fuller, J. Gray, M. H. Holmes and G. J. T. Tiddy, in *Handbook of Liquid Crystals*, ed. D. Demus, J. Goodby, G. W. Gray, H.-W. Spiess and V. Vill, Wiley-VCH, New York, 1998, vol. 3, p. 341.
- 2 G. S. Kwon and T. Okano, *Adv. Drug Delivery Rev.*, 1996, **21**, 107.
- 3 B. Chu and Z. Zhou in *Surfactant science series Vol. 60: Nonionic surfactants: polyoxyalkylene block copolymers*, ed. V. M. Nace and M. Dekker, New York, 1996, ch. 3.
- 4 K. Mortensen and Y. Talmon, *Macromolecules*, 1995, **28**, 8829.
- 5 G.-E. Yu, Y. Deng, S. Dalton, Q.-G. Wang, D. Attwood, C. Price and C. Booth, *J. Chem. Soc., Faraday Trans.*, 1992, **88**, 2537.
- 6 D. E. Bradley, in *Techniques for electron microscopy*, ed. D. Kay, Blackwell Scientific Publications, Oxford and Edinburgh, 1965, p. 58.
- 7 J. Dubochet, M. Adrian, J.-J. Chang, J.-C. Homo, J. Lepault, A. W. McDowell and P. Schultz, *Q. Rev. Biophys.*, 1988, **21**, 129.
- 8 J. R. Bellare, H. T. Davis, L. E. Scriven and Y. Talmon, *J. Electron Microsc. Tech.*, 1988, **10**, 87.
- 9 W. O. Saxton, T. J. Pitt and M. Horner, *Ultramicroscopy*, 1979, **4**, 343.
- 10 P. Alexandridis, U. Olsson and B. Lindmann, *Macromolecules*, 1995, **28**, 7700.
- 11 H. Fischer, TNO Eindhoven (NL), private communication of GPC analysis.

Paper 9/02369K